

## Self-Assembly of a Tripodal Pseudorotaxane on the Surface of a Titanium Dioxide Nanoparticle

Brenda Long, Kirill Nikitin, and Donald Fitzmaurice\*

Contribution from the Department of Chemistry, University College Dublin, Belfield, Dublin 4, Ireland

Received October 9, 2002; Revised Manuscript Received February 4, 2003; E-mail: donald.fitzmaurice@ucd.ie

**Abstract:** This paper describes the self-assembly of a heterosupramolecular system consisting of a tripodal viologen, adsorbed at the surface of a titanium dioxide nanoparticle, that threads a crown ether to form a pseudorotaxane. The viologen, a 1,1'-disubstituted-4,4'-bipyridinium salt with a rigid tripodal anchor group, has been synthesized. This viologen is adsorbed at the surface of a titanium dioxide nanoparticle in solution. As intended, this tripodal viologen is both oriented normal to and displaced from the surface of the nanoparticle and threads a crown ether to form the heterosupramolecular complex. The threading of the crown ether by the tripodal viologen to form the above pseudorotaxane complex at the surface of a titanium dioxide nanoparticle has been studied by <sup>1</sup>H NMR, optical absorption spectroscopy, and cyclic voltammetry.

### Introduction

The bottom-up assembly of functional nanoscale architectures in solution is a goal shared by researchers in many fields.<sup>1</sup> Expected benefits include greater control over material properties and innovative technologies that address unmet needs.<sup>2</sup> One approach envisaged is the self-assembly of nanoscale architectures from molecular and condensed-phase components in solution and at a surface.<sup>3</sup>

In considering what molecular and condensed-phase components might be suitable,<sup>4–6</sup> one is immediately attracted to functional supermolecules<sup>7</sup> and to the rapidly growing number of nanoparticles whose properties can be tuned by controlling their size and surface composition.<sup>8</sup> It is in this context that we have sought to synthesize molecular components that are adsorbed at the surface of a nanoparticle, orientated normal to the surface of the nanoparticle in order to allow their self-assembly to form a supermolecule, displaced from the nanoparticle in order to avoid unwanted surface effects, and finally, sufficiently bulky to preclude unwanted lateral interactions.

A class of functional supermolecule that has attracted a great deal of attention is the pseudorotaxanes.<sup>9</sup> A class of nanoparticle that has attracted a great deal of attention is metal oxides.<sup>10</sup>

Accordingly, we have designed and synthesized the tripodal viologen **9** shown in Scheme 1. The phosphonate linkers

strongly bind the viologen to the surface of a titanium dioxide nanoparticle. The rigid tripodal arrangement of the linkers orients the viologen normal to and displaces it from the surface of the nanoparticle. The inherent bulkiness of the viologen reduces the possibility of pimerization of the reduced viologen.<sup>11</sup> As a consequence, the tripodal viologen **9** complexes the crown ether **10** at the surface of the titanium dioxide nanoparticle to form a heteropseudorotaxane **9**·**10** shown in Scheme 1.

It should be noted that Fitzmaurice and co-workers<sup>12</sup> have recently described the synthesis of a long-chain alkane thiol incorporating a terminal crown moiety that is capable of being adsorbed at the surface of a gold nanoparticle and of threading a dibenzylammonium cation to form a pseudorotaxane.

It should also be noted that Galoppini and co-workers<sup>13</sup> have recently described the synthesis of tripodal linkers used to adsorb sensitizer molecules at the surface of the constituent titanium dioxide nanoparticles of a nanostructured film, forming the anode of a regenerative photoelectrochemical cell.

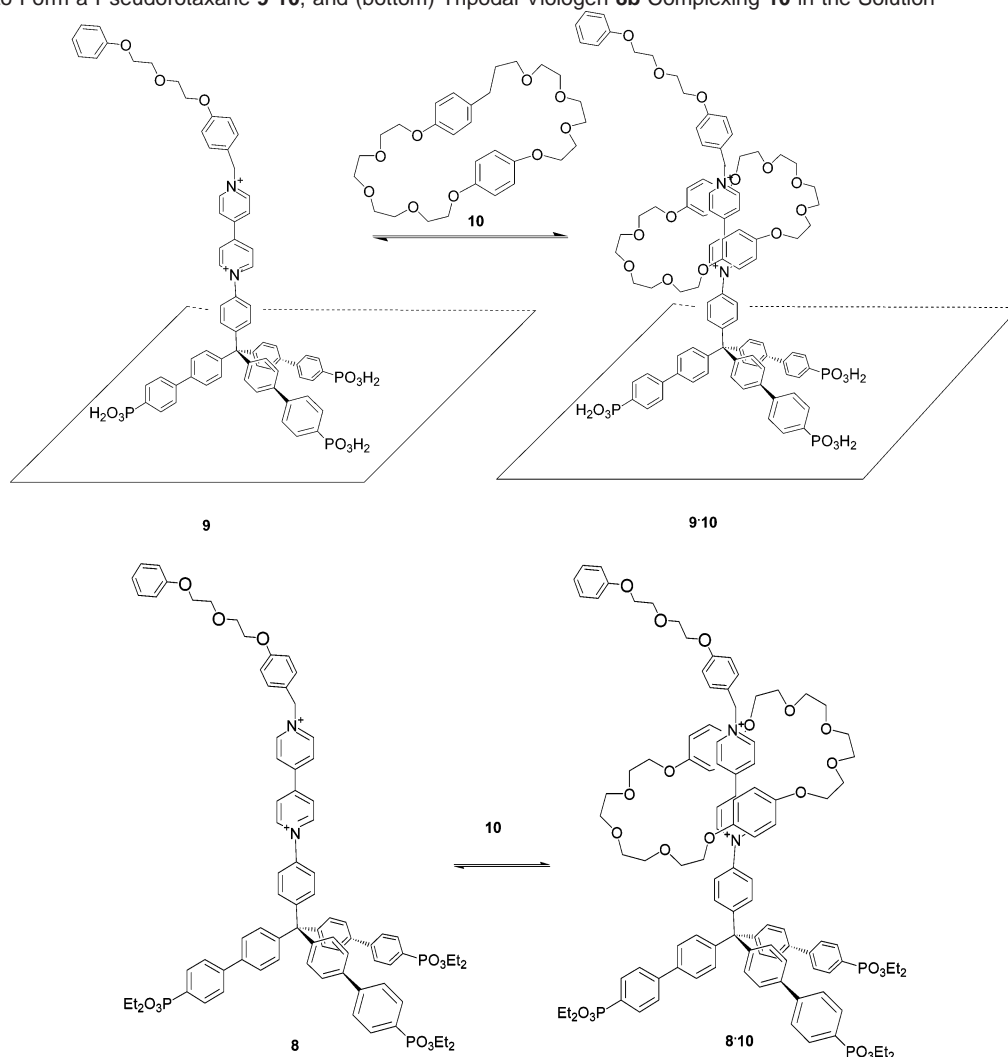
### Results and Discussion

**Design and Synthesis of Molecular Components.** The synthesis of the tripodal viologen **9** was largely based on known transformations and followed the synthetic strategy outlined in Scheme 2. The key to the success of this strategy was minimizing the interaction between any peripheral substituents and the tertiary carbon in the triarylmethyl alcohol **2**. Toward this end, each leg of molecular tripod was constructed from

- (1) Philp, D.; Stoddart, J. F. *Angew. Chem., Int. Ed. Engl.* **1996**, *35*, 1154–1196.
- (2) Bows, W. *Investors Chronicle* **2002**, *139*, 30–32.
- (3) Whitesides, G. M.; Mathias, J. P.; Seto, C. T. *Science* **1991**, *254*, 1212–1319.
- (4) Service, R. F. *Science* **1997**, *277*, 1036–1037.
- (5) Mann, S.; Shenton, W.; Li, M.; Connolly, S.; Fitzmaurice, D. *Adv. Mater.* **2000**, *12*, 147–150.
- (6) Niemeyer, C. *Angew. Chem., Int. Ed.* **2001**, *40*, 4128.
- (7) Lehn, J.-M. *Supramolecular Chemistry, Concepts and Perspectives*; VCH: Weinheim, Germany, 1995.
- (8) Alivisatos, A. P. *Science* **1996**, *271*, 933–937.
- (9) Ashon, P. R.; Glink, P. T.; Stoddart, J. F.; Tasker, P. A.; White, A. J. P.; Williams, D. *Chem. Eur. J.* **1996**, *2*, 729.
- (10) Hagfeldt, A.; Gratzel, M. *Chem. Rev.* **1995**, *95*, 49.

- (11) Felderhoff, M.; Heinen, S.; Molisho, N.; Webersinn, S.; Walder, L. *Helv. Chim. Acta* **2000**, *83*, 181.
- (12) (a) Fitzmaurice, D.; Rao, S. N.; Preece, J. A.; Stoddart, J. F.; Wenger, S.; Zacccheroni, N. *Angew. Chem., Int. Ed.* **1999**, *38*, 1147. (b) Ryan, D.; Rao, S. N.; Rensmo, H.; Fitzmaurice, D.; Preece, J. A.; Wenger, S.; Stoddart, J. F.; Zacccheroni, N. *J. Am. Chem. Soc.* **2000**, *122*, 6252. (c) Chia, S.; Cao, J.; Stoddart, J. F.; Zink, J. I. *Angew. Chem., Int. Ed.* **2001**, *40*, 2447.
- (13) (a) Galoppini, E.; Guo, W. *J. Am. Chem. Soc.* **2001**, *123*, 4342. (b) Galoppini, E.; Guo, W.; Zhang, W.; Hoetz, P. G.; Qu, P.; Meyer, G. J. *J. Am. Chem. Soc.* **2002**, *124*, 7801.

**Scheme 1.** (Top) Tripodal Viologen **9** Adsorbed Normal to and Displaced from the Surface of a Titanium Dioxide Nanoparticle and Complexing **10** to Form a Pseudorotaxane **9·10**, and (bottom) Tripodal Viologen **8b** Complexing **10** in the Solution



two *p*-phenylene groups. This allowed the triarylmethyl derivative of aniline **3** to be prepared from **2** due to a relatively weak influence of tertiary carbon on the terminal halogen functional groups.

The alcohol **2** was prepared from 4,4'-dibromobiphenyl in a high-yield step that involved lithiation followed by nucleophilic addition of the resulting intermediate 4-(4-bromophenyl)phenyllithium to diethyl carbonate.<sup>14</sup> The alcohol **2** was successfully converted into the aniline derivative **3** by a known electrophilic alkylation procedure in acetic acid.<sup>15</sup> To convert the amine **3** into the ester **4**, a palladium-catalyzed substitution was carried out. The conditions were similar to those previously reported,<sup>16</sup> but a more suitable catalyst was employed. To prepare the monocation **6**, an elegant procedure that used the bipyridinium salt **5** was applied.<sup>17</sup> In the course of this ring opening–closure reaction, the nitrogen atom of **5** is displaced by a nitrogen originating from the ester **4**.

The alkylation of **6** with EtBr (**7a**) proceeds in acetonitrile in high yield. Alkylation with reagent **7b**, structurally similar to the well-known stopper groups, proceeds in benzonitrile with high yield.<sup>18</sup>

The products **8a** or **8b** were isolated in the form of a  $\text{Cl}^-$  or  $\text{PF}_6^-$  salt, respectively. The hexafluorophosphate salts of **8a** or **8b** were used for measurements made in solution and for the subsequent transformation into corresponding phosphonic acid **9**.

**Formation of Pseudorotaxanes in Solution.** Threading of the crown ether **10** by the tripodal viologen **8b**· $2\text{PF}_6$  to form the pseudorotaxane **8b**·**10**· $2\text{PF}_6$  is shown in Scheme 1. Complexation is accompanied by characteristic changes in the measured  $^1\text{H}$  NMR spectra, optical absorption spectra, and cyclic voltammograms (Figure 1).

The  $^1\text{H}$  NMR spectra (expansion of the bipyridinium proton signal range) of the viologen **8b**· $2\text{PF}_6$  ( $5 \times 10^{-3}$  mol  $\text{dm}^{-3}$ ), the crown ether **10** ( $5 \times 10^{-3}$  mol  $\text{dm}^{-3}$ ) and the corresponding 1:1 **8b**·**10**· $2\text{PF}_6$  complex ( $5 \times 10^{-3}$  mol  $\text{dm}^{-3}$  each component) are shown in the top panel of Figure 1. Pronounced changes in the chemical shifts of the protons in the 3 and 3' positions of 4,4'-bipyridinium dication, as well as less pronounced changes for the protons in the 2 and 2' positions, are observed.<sup>19</sup>

(16) Gonzalez-Bello, C.; Abell, C.; Leeper, F. J. *J. Chem. Soc., Perkin. Trans. 1* **1997**, 1017.

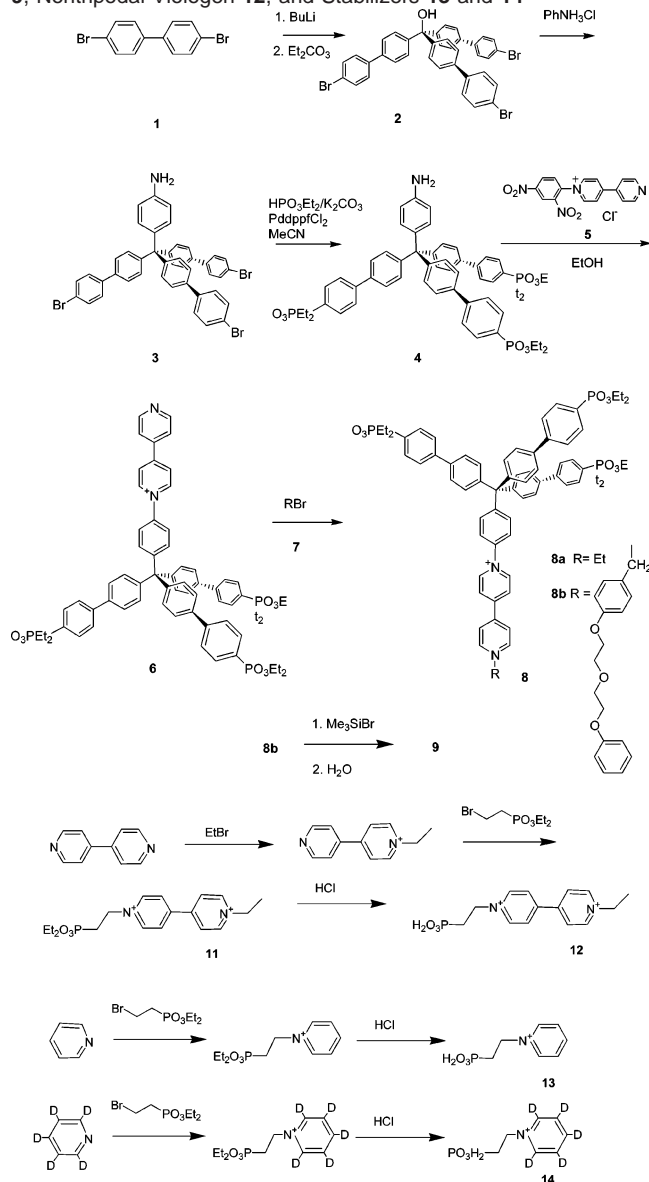
(17) Hanke, M.; Lutz, C. *Synthesis* **1980**, 31.

(18) Ashton, P. R.; Philp, D.; Spencer, N.; Stoddart, J. F. *J. Chem. Soc., Chem. Commun.* **1992**, 1124.

(14) Chen, L. S.; Chen, G. J.; Tamborski, C. *J. Organomet. Chem.* **1983**, 251, 139.

(15) *Organic Syntheses*; Wiley: New York, 1955; Collect. Vol. III, 47.

**Scheme 2.** Synthetic Scheme for Preparation of Tripodal Viologen **9**, Nontripodal Viologen **12**, and Stabilizers **13** and **14**



The optical absorption spectra of the viologen **8b**·2PF<sub>6</sub> ( $2 \times 10^{-4}$  mol dm<sup>-3</sup>), in the absence and presence of the crown ether **10** ( $1 \times 10^{-3}$  mol dm<sup>-3</sup>), are shown in the middle panel of Figure 1. The difference between the spectra measured for the corresponding 1:1 **8b**·**10**·2PF<sub>6</sub> complex and the viologen **8b**·2PF<sub>6</sub> is plotted and indicates the presence of a charge-transfer absorption band at 390 nm with a shoulder at 480 nm.<sup>20</sup>

The corresponding cyclic voltammograms of the viologen **8b**·2PF<sub>6</sub> ( $1 \times 10^{-3}$  mol dm<sup>-3</sup>), in the absence and presence of the crown ether **10** ( $5 \times 10^{-3}$  mol dm<sup>-3</sup>) are shown in the bottom panel of Figure 1. It is clear that the first peak reduction potential of the viologen is shifted to more negative potentials by 41 mV in the presence of the added crown.<sup>21</sup> The corresponding oxidation potential is also shifted to more negative potentials by 35 mV.

- (19) Allwood, B. L.; Spencer, N.; Shahriari-Zavareh, H.; Stoddart, J. F.; Williams, D. J. *J. Chem. Soc., Chem. Commun.* **1987**, 1064.  
 (20) Steed, J. W.; Atwood, J. L. *Supramolecular Chemistry*; Wiley: New York, 2000.  
 (21) Ashton, P. R.; Ballardini, R.; Balzani, V.; Credi, A.; Ruprecht-Dress, K.; Ishow, E.; Kleverlaan, C.; Kocian, O.; Preece, J.; Spencer, N.; Stoddart, J. F.; Venturi, M.; Wenger, S. *Chem. Eur. J.* **2000**, *6*, 3558.

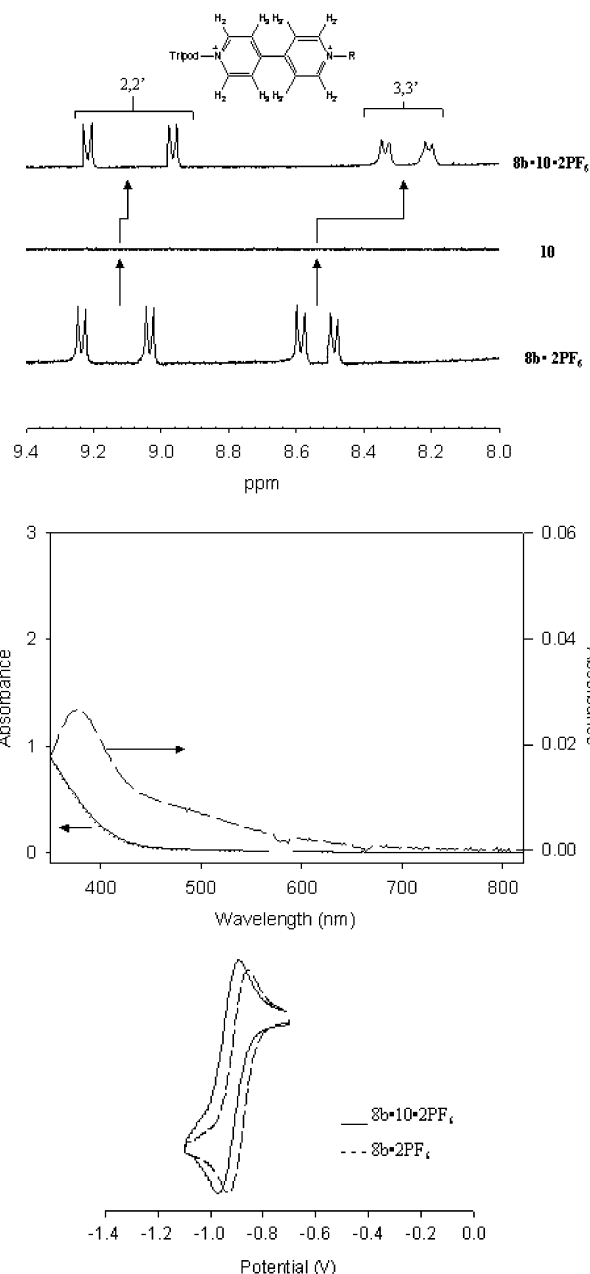


**Figure 1.** (Top panel) <sup>1</sup>H NMR spectra of **8b**·2PF<sub>6</sub> ( $5 \times 10^{-3}$  mol dm<sup>-3</sup>), **10** ( $5 \times 10^{-3}$  mol dm<sup>-3</sup>), and an equimolar mixture of **8b**·2PF<sub>6</sub> and **10** ( $5 \times 10^{-3}$  mol dm<sup>-3</sup> each) in acetonitrile at 30 °C. (Middle panel) Optical absorption spectra of (···) **8b**·2PF<sub>6</sub> ( $2 \times 10^{-4}$  mol dm<sup>-3</sup>), a mixture (—) of **8b**·2PF<sub>6</sub> ( $2 \times 10^{-4}$  mol dm<sup>-3</sup>) and **10** ( $1 \times 10^{-3}$  mol dm<sup>-3</sup>), and the difference (---) of these two spectra in acetonitrile at 25 °C. (Bottom panel) Cyclic voltammograms of (---) **8b**·2PF<sub>6</sub> ( $1 \times 10^{-3}$  mol dm<sup>-3</sup>) and a mixture (—) of **8b**·2PF<sub>6</sub> ( $1 \times 10^{-3}$  mol dm<sup>-3</sup>) and **10** ( $5 \times 10^{-3}$  mol dm<sup>-3</sup>) in methanol at 25 °C.

The complexation of the nontripodal viologen **11**·2Br with crown ether **10** to form the pseudorotaxane **11**·**10**·2Br was also studied. As above, complexation is accompanied by changes in the measured <sup>1</sup>H NMR spectra, optical absorption spectra, and cyclic voltammograms (Figure 2).

The <sup>1</sup>H NMR spectra (expansion of the bipyridinium proton signal range) of the viologen **11**·2Br ( $5 \times 10^{-3}$  mol dm<sup>-3</sup>), the crown ether ( $5 \times 10^{-3}$  mol dm<sup>-3</sup>), and the corresponding 1:1 **11**·**10**·2Br complex ( $5 \times 10^{-3}$  mol dm<sup>-3</sup> each component) are shown in the top panel of Figure 2. The resonances assigned to the protons at the 3 and 3' positions of 4,4'-bipyridinium are

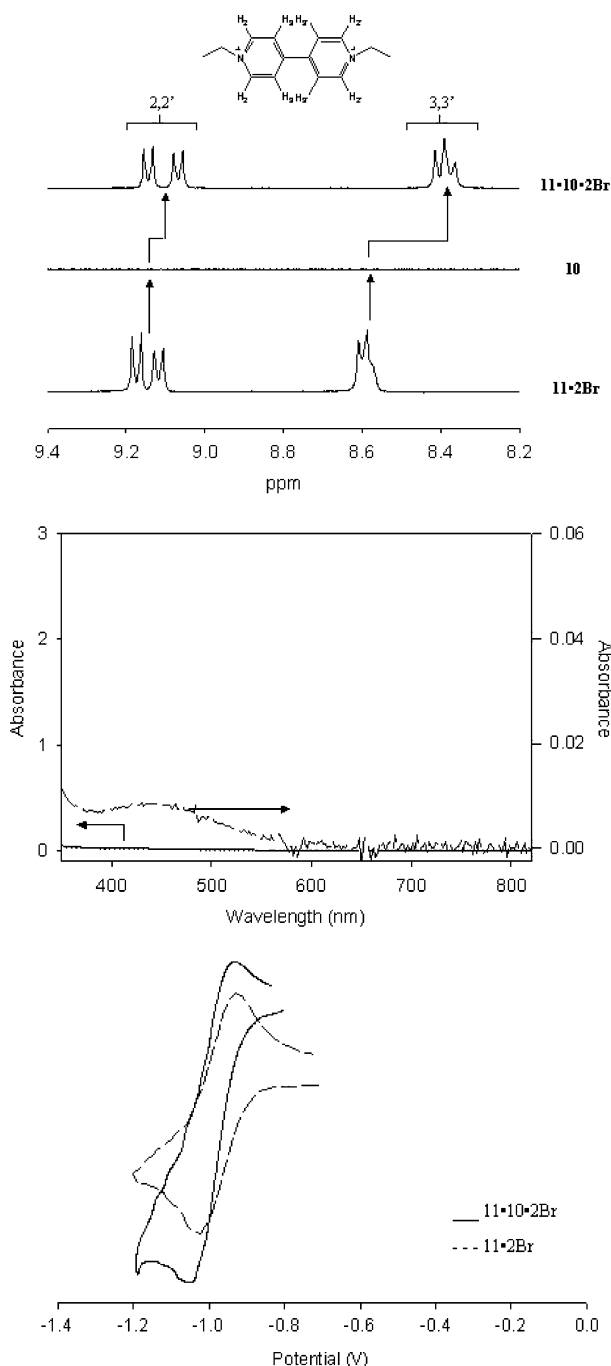


**Figure 2.** (Top panel) <sup>1</sup>H NMR spectra of **11·2Br** ( $5 \times 10^{-3}$  mol dm<sup>-3</sup>), **10** ( $5 \times 10^{-3}$  mol dm<sup>-3</sup>), and an equimolar mixture of **11·2Br** and **10** ( $5 \times 10^{-3}$  mol dm<sup>-3</sup> each) in acetonitrile at 30 °C. (Middle panel) Optical absorption spectra of (···) **11·2Br** ( $2 \times 10^{-4}$  mol dm<sup>-3</sup>), a mixture (—) of **11·2Br** ( $2 \times 10^{-4}$  mol dm<sup>-3</sup>) and **10** ( $1 \times 10^{-3}$  mol dm<sup>-3</sup>), and the difference (---) of these two spectra in acetonitrile at 25 °C. (Bottom panel) Cyclic voltammograms of (---) **11·2Br** ( $1 \times 10^{-3}$  mol dm<sup>-3</sup>) and a mixture (—) of **11·2Br** ( $1 \times 10^{-3}$  mol dm<sup>-3</sup>) and **10** ( $5 \times 10^{-3}$  mol dm<sup>-3</sup>) in methanol at 25 °C.

shifted significantly, while those assigned to the protons at 2 and 2' positions show smaller shifts.<sup>19</sup>

The optical absorption spectra of the viologen **11·2Br** ( $2 \times 10^{-4}$  mol dm<sup>-3</sup>) with and without the crown ether **10** ( $1 \times 10^{-3}$  mol dm<sup>-3</sup>) are shown in the middle panel of Figure 2. The corresponding difference spectrum indicates the presence of a charge-transfer absorption band at 444 nm.<sup>20</sup>

**Table 1.** Association Constants and Derived Free Energies for Formation of a Viologen–Crown Complex at 25 °C

viologen	solvent	$K_a$ (M <sup>-1</sup> )	$\Delta G^\circ$ (kcal mol <sup>-1</sup> )
<b>8b·2PF<sub>6</sub></b>	MeOH/CHCl <sub>3</sub>	1243 ± 20	-4.203
<b>8b·2PF<sub>6</sub></b>	MeCN	795 ± 16	-3.940
<b>8b·2Cl<sub>2</sub></b>	MeOH/CHCl <sub>3</sub>	650 ± 8	-3.821
<b>11·2Br</b>	MeOH/CHCl <sub>3</sub>	139 ± 5	-3.83

The corresponding cyclic voltammograms of the viologen **11·2Br** ( $1 \times 10^{-3}$  mol dm<sup>-3</sup>), in the absence and presence of the crown ether **10** ( $5 \times 10^{-3}$  mol dm<sup>-3</sup>), are shown in the bottom panel of Figure 2. It is clear that the first peak reduction potential of the viologen is shifted to more negative potentials by 30 mV in the presence of the added crown.<sup>21</sup> The corresponding oxidation potential is shifted to more negative potentials by only 3 mV.

These findings are accounted for by the electron-deficient viologens forming a stable colored complex with the electron-rich crown ether. As a result there is a transfer of electron density to the viologen from the crown. The stabilizing interactions include a  $\pi$ - $\pi$  charge transfer between the electron-deficient 1,1'-quaternized pyridinium rings of the viologen and the electron-rich *p*-phenylene rings of the crown. This stabilization is reinforced by a  $\delta^+$ - $\delta^-$  electrostatic interaction between the positive nitrogens in the viologen and the electronegative oxygens in the crown. The pseudorotaxane may be further stabilized by H-bonding between the 2- and 2'-hydrogens of the bipyridinium and the oxygens of the crown ether.

Quantifying the collective strength of these noncovalent interactions requires that the association constant,  $K_a$ , for the complex be determined. The spectrophotometric method used to determine  $K_a$  was that developed by Ray and adapted by Stoddart for pseudorotaxanes.<sup>22,23</sup> The association constants  $K_a$  and derived values for the change in free energy  $\Delta G^\circ$  are recorded in Table 1. It is evident that the  $K_a$  for the tripodal viologen, **8b·2PF<sub>6</sub>** in acetonitrile, and both **8b·2PF<sub>6</sub>** and **8b·2Br** in methanol/chloroform (1:1 by volume), are substantially higher than for the simple viologen **11·2Br** in methanol/chloroform (1:1 by volume). Since **8b** has a phenyl ring conjugated to the viologen, it is possible that this phenyl ring, linking the tripod moiety to the viologen, allows the crown ether **10** to adopt a more energetically stable conformation within the complex formed than is the case for the complex formed with **11·2Br**. It is also possible that the long-chain (phenoxy-ethoxy)ethoxy group hinders dissociation of **8b·10·2PF<sub>6</sub>**.

Consistent with this finding, it is concluded in the case of **8b·10·2PF<sub>6</sub>** that, following reduction of the pseudorotaxane, the crown remains associated, albeit more weakly, with the radical cation of the viologen. This accounts for the finding that both the first reduction potential and the corresponding oxidation potential of the viologen are shifted to more negative potentials. It is also concluded in the case of **11·10·2Br** that, following reduction of the pseudorotaxane, the complex dissociates fully. This accounts for the finding that while the first reduction potential is shifted to more negative potentials, the corresponding oxidation potential is not.<sup>21</sup>

**Adsorption of Viologens at the Surface of a Nanoparticle.** It has been established that both the tripodal viologen **8b·2PF<sub>6</sub>**

(22) Ray, A. *J. Am. Chem. Soc.* **1971**, *93*, 7146.

(23) Colquhoun, H. M.; Goodings, E. P.; Stoddart, J. F.; Wohlstenholme, J. B.; Williams, D. J. *J. Chem. Soc., Perkin Trans 2* **1985**, 607.

and nontripodal viologen **11**·2Br thread the crown ether **10** to form a pseudorotaxane in solution. What remains to be established is whether, as expected, the tripodal viologen **9**·2PF<sub>6</sub> (acid analogue of **8b**·2PF<sub>6</sub>) threads the crown ether **10** to form a pseudorotaxane when adsorbed at the surface of a titanium dioxide nanoparticle. It is not expected that the nontripodal viologen **12**·2PF<sub>6</sub> (acid analogue of **11**·2Br) will do so.

A charge-stabilized dispersion of titanium dioxide nanoparticles (5 nm diameter) was prepared by hydrolysis of titanium orthotetraisopropoxide in water at pH 2.<sup>24</sup> The tripodal viologen **9**·2Br readily chelates surface Ti<sup>4+</sup> sites and is adsorbed at the surface of the above nanoparticles. The number of Ti<sup>4+</sup> sites on the surface of each nanoparticle was estimated, on the basis of literature values for the number of such sites ( $2 \times 10^{14}$  cm<sup>-2</sup>), to be 160.<sup>25</sup> An average of 13 viologens **9**·2Br or 39 **12**·2Cl, occupying 39 or 13 of the available sites, respectively, were adsorbed at the surface of each titanium dioxide nanoparticle. Structurally similar stabilizer molecules, 1-(2-phosphoethyl)pyridinium bromide (**13**) or a partially deuterated analogue, namely, 1-(2-phosphoethyl)pyridinium-*d*<sub>5</sub> bromide (**14**), were adsorbed at the remaining Ti<sup>4+</sup> sites on the surface of each nanoparticle. The above nanoparticles were precipitated by addition of ammonium hexafluorophosphate, washed with dry methanol, and redispersed in acetonitrile to form a stable optically transparent dispersion. The concentrations of nanoparticles given below are in moles of particles per cubic decimeter.

**Formation of Pseudorotaxanes on the Surface of a Titanium Dioxide Nanoparticle.** Titanium dioxide nanoparticles modified by the adsorption of the viologen **9**·2PF<sub>6</sub> or **12**·2PF<sub>6</sub> and stabilized by the adsorption of **13** or **14** were studied by <sup>1</sup>H NMR, optical absorption spectroscopy, and cyclic voltammetry in the absence and presence of the crown ether **10**.

The tripodal viologen **9**·2PF<sub>6</sub> ( $2 \times 10^{-3}$  mol dm<sup>-3</sup>) was adsorbed at the surface of titanium dioxide nanoparticles ( $1.5 \times 10^{-4}$  mol dm<sup>-3</sup>). The <sup>1</sup>H NMR spectra of **9**·2PF<sub>6</sub> adsorbed at the surface of the above nanoparticles, in the absence and presence of a 5-fold excess of **10** ( $1 \times 10^{-2}$  mol dm<sup>-3</sup>), and of **8b**·2PF<sub>6</sub> ( $5 \times 10^{-3}$  mol dm<sup>-3</sup>) in solution are shown in the top panel of Figure 3. It should be noted that the partially deuterated stabilizer **14** was used in the preparation of these nanoparticles as it provided the required spectroscopic window.

It is clear that the tripodal viologen **9**·2PF<sub>6</sub> is adsorbed at the surface of the titanium dioxide nanoparticle. That this is the case may be deduced from the reduction in intensity and broadening of the resonances assigned to protons in **9**·2PF<sub>6</sub>.

Specifically, the following resonances are significantly reduced in intensity and broadened:  $\delta$  9.3 (the 2 position of 4,4'-bipyridinium), 9.2 (the 2' position of 4,4'-bipyridinium), 8.6 (the 3 position of 4,4'-bipyridinium), 8.5 (the 3' position of 4,4'-bipyridinium), 7.9–7.8 (phosphorylated *p*-phenylenes of tripod legs and *p*-phenylene link to bipyridinium), 7.7 (*p*-phenylene of tripod legs), 7.5 (*p*-phenylene of tripod legs and the 3-position of N-benzyl), 7.1 (the 2 position of N-benzyl), and 5.6 (methylene of N-benzyl). The reason these resonances are reduced in intensity and broadened is due in part to a

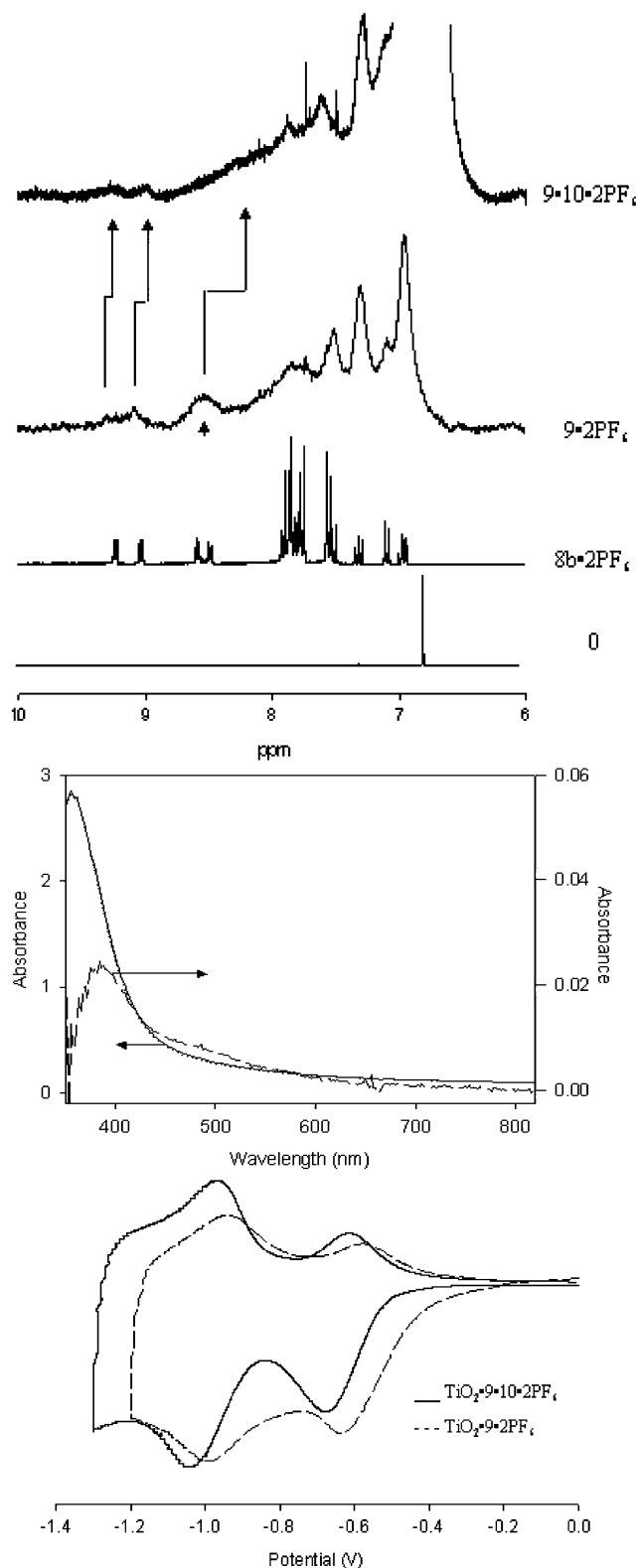


**Figure 3.** (Top panel) <sup>1</sup>H NMR spectra of **8b**·2PF<sub>6</sub> ( $5 \times 10^{-3}$  mol dm<sup>-3</sup>) in solution and **9**·2PF<sub>6</sub> ( $2 \times 10^{-3}$  mol dm<sup>-3</sup>) on titanium dioxide nanoparticles ( $1.5 \times 10^{-5}$  mol dm<sup>-3</sup>), in the absence and presence of added **10** ( $1 \times 10^{-2}$  mol dm<sup>-3</sup>) in acetonitrile at 30° C. (Middle panel) Optical absorption spectra of (—) a mixture of **9**·2PF<sub>6</sub> ( $2 \times 10^{-4}$  mol dm<sup>-3</sup>) on titanium dioxide nanoparticles ( $1.5 \times 10^{-5}$  mol dm<sup>-3</sup>) with **10** ( $1 \times 10^{-3}$  mol dm<sup>-3</sup>), (···) of **9**·2PF<sub>6</sub> ( $2 \times 10^{-4}$  mol dm<sup>-3</sup>) on titanium dioxide nanoparticles ( $1.5 \times 10^{-5}$  mol dm<sup>-3</sup>), and the difference (— —) of these two spectra in acetonitrile at 25° C. (Bottom panel) Cyclic voltammograms of **9**·2PF<sub>6</sub> ( $6 \times 10^{16}$  molecules cm<sup>-2</sup>) in the presence (—) and absence (— —) of **10** ( $1 \times 10^{-2}$  mol dm<sup>-3</sup>) in acetonitrile at 25° C.

(24) O'Reagen, B.; Graetzel, M. *Nature* **1991**, *353*, 737.

(25) Finklea, H. O. *Semiconductor Electrodes*; Elsevier: Amsterdam, 1988.

discontinuity in the paramagnetic susceptibility at the surface of the titanium dioxide nanoparticle and in part to the restricted motion of the immobilized tripodal viologen.<sup>26</sup>

By comparison, the following resonances are not significantly reduced in intensity or broadened:  $\delta$  7.3 (the 3 position of terminal phenyl), 6.9–7.0 (the 2 and 4 positions of the terminal phenyl), 4.1 (ether link positions adjacent to aryloxy groups), and 3.9 (rest of ether link positions). The reason these resonances largely persist is that the long-chain (phenoxyethoxy)ethoxy moiety attached to the viologen is both sufficiently far from the nanoparticle surface and free to rotate.

The proton resonances, which are observed to shift upon complexation of the crown ether **10** by the tripodal viologen **8b**·2PF<sub>6</sub> in solution (Figure 1, top panel), are those assigned to the protons in the 3,3' and 2,2' positions of the 4,4'-bipyridinium moiety. What is clear from the findings presented here is that similar shifts are observed upon complexation of the crown ether **10** by the tripodal viologen **9**·2PF<sub>6</sub> adsorbed at the surface of a TiO<sub>2</sub> nanoparticle (Figure 3, top panel). It should be noted that these shifts could only be observed by use of the partially deuterated stabilizer **14**.

The optical absorption spectra of the tripodal viologen **9**·2PF<sub>6</sub> ( $2 \times 10^{-4}$  mol dm<sup>-3</sup>) adsorbed at the surface of a titanium dioxide nanoparticle ( $1.5 \times 10^{-5}$  mol dm<sup>-3</sup>), in the absence and presence of the crown ether **10** ( $1 \times 10^{-3}$  mol dm<sup>-3</sup>), are shown in the middle panel of Figure 3. The resulting difference spectrum is similar to that measured for the ester analogue **8b**·2PF<sub>6</sub> and the crown ether **10** (Figure 1, middle panel).

The corresponding cyclic voltammograms of the viologen **9**·2PF<sub>6</sub> ( $6 \times 10^{16}$  molecules cm<sup>-2</sup>) adsorbed at the surface of the constituent TiO<sub>2</sub> nanoparticles of a nanostructured film, in the absence and presence of the crown ether **10** ( $1 \times 10^{-2}$  mol dm<sup>-3</sup>), are shown in the bottom panel of Figure 3. It is found that the first and second peak reduction potentials of the viologen are shifted to more negative values by 44 and 48 mV, respectively, in the presence of the added crown. It is also found that the first and second peak oxidation potentials are shifted to more negative values by 25 and 26 mV in the presence of added crown.

On this basis it is concluded that the tripodal viologen **9**·2PF<sub>6</sub> adsorbed at the surface of a titanium dioxide nanoparticle threads the crown ether **10** to form a heteropseudorotaxane. It is also concluded that transfer of an electron to the viologen to form the corresponding radical cation does not result in dissociation of the heteropseudorotaxane at the surface.

It has not been possible to accurately determine  $K_a$  for the complex **9**·**10**·2PF<sub>6</sub> formed at the surface of a titanium dioxide nanoparticle. This is because, at the nanoparticle concentrations used, the sample is not sufficiently transparent. However, it can be reasonably assumed that the  $K_a$  is similar to that measured in acetonitrile for **8b**·2PF<sub>6</sub> ( $795 \pm 16$  mol<sup>-1</sup> dm). The fact that the magnitude of the charge-transfer absorption assigned to the formation of complex is similar, as shown in the middle panels of Figures 1 (0.027) and 2 (0.024), supports that assumption.

The corresponding <sup>1</sup>H NMR and optical absorption spectra of nontripodal viologen **12**·2PF<sub>6</sub> on titanium dioxide nanoparticles were measured. The <sup>1</sup>H NMR spectrum of **12**·2PF<sub>6</sub>

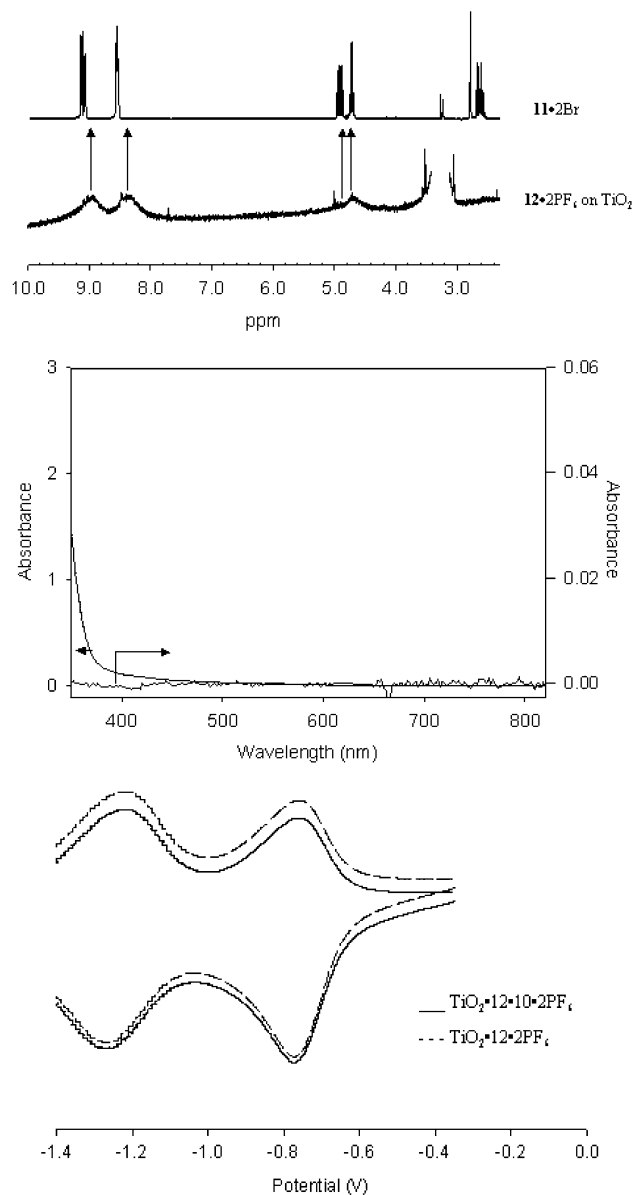


**Figure 4.** (Top panel) <sup>1</sup>H NMR spectra of **11**·2Br ( $5 \times 10^{-3}$  mol dm<sup>-3</sup>) in solution and **12**·2PF<sub>6</sub> ( $2 \times 10^{-3}$  mol dm<sup>-3</sup>) on titanium dioxide nanoparticles ( $1.5 \times 10^{-5}$  mol dm<sup>-3</sup>), in the absence and presence (not shown) of added **10** ( $1 \times 10^{-2}$  mol dm<sup>-3</sup>) in acetonitrile at 30° C. (Middle panel) Optical absorption spectra of (—) a mixture of **12**·2PF<sub>6</sub> ( $2 \times 10^{-4}$  mol dm<sup>-3</sup>) on titanium dioxide nanoparticles ( $1.5 \times 10^{-5}$  mol dm<sup>-3</sup>) with **10** ( $1 \times 10^{-3}$  mol dm<sup>-3</sup>), (···) **12**·2PF<sub>6</sub> ( $2 \times 10^{-4}$  mol dm<sup>-3</sup>) on titanium dioxide nanoparticles ( $1.5 \times 10^{-5}$  mol dm<sup>-3</sup>), and the difference (---) of these two spectra in acetonitrile at 25° C. (Bottom panel) Cyclic voltammograms of **12**·2PF<sub>6</sub> ( $6 \times 10^{16}$  molecules cm<sup>-2</sup>) in the presence (—) and absence (---) of **10** ( $1 \cdot 10^{-2}$  mol dm<sup>-3</sup>) in acetonitrile at 25° C.

( $2 \times 10^{-3}$  mol dm<sup>-3</sup>) adsorbed on the nanoparticles ( $1.5 \times 10^{-4}$  mol dm<sup>-3</sup>) and <sup>1</sup>H NMR spectrum of the free **12**·2Br ( $5 \times 10^{-3}$  mol dm<sup>-3</sup>) are shown in the top panel of Figure 4. It should be noted that the partially deuterated stabilizer **14** was used in the preparation of the nanoparticle dispersion, as it again provided the required spectroscopic window.

It is clear from the top panel of Figure 4 that the viologen **12**·2PF<sub>6</sub> is adsorbed at the surface of the titanium dioxide nanoparticle. This has been deduced from the significant reduction in intensity and broadening of the proton resonances. Specifically, the following resonance is not observed at the

(26) Korgel, B. A.; Fullan, S.; Connolly, S.; Fitzmaurice, D. J. *Phys. Chem.* **1998**, *102*, 8379.

surface:  $\delta$  2.6 (the methylene group  $\alpha$  to the phosphonic acid). By comparison, the following resonances, although significantly reduced in intensity and broadened, are observed:  $\delta$  9.0 (the 2 and 2' positions of 4,4'-bipyridinium), 8.4 (the 3 and 3' positions of 4,4'-bipyridinium), 4.95 (the methylene group  $\beta$  to the phosphonic acid), 4.7 (the methylene group of the terminal ethyl), and 1.7 (methyl of the terminal ethyl, not shown in Figure 4, top panel). Significantly, addition of the crown **10** ( $2 \times 10^{-3}$  mol dm $^{-3}$ ) to the above dispersion does not result in any measured change in the spectrum for **12**·2PF $_6$  adsorbed at the surface of the titanium dioxide nanoparticle (Figure 4, top panel). This finding suggests that the corresponding heteropseudorotaxane is not formed.

It is interesting to note that the proton resonances assigned to the viologen moiety of **12**·2PF $_6$ , although significantly reduced in intensity and broadened, persist in the  $^1\text{H}$  NMR spectrum of this molecule adsorbed at the surface of a TiO $_2$  nanoparticle. This is comparable behavior to that observed for the proton resonances assigned to the viologen moiety in **9**·2PF $_6$ . This would suggest that the viologen moiety of **12**·2PF $_6$  is not adsorbed flat at the surface of the nanoparticle, as might have been expected to be the case with a nontripodal phosphonate linker.

The optical absorption spectrum of the nontripodal viologen **12**·2PF $_6$  ( $2 \times 10^{-4}$  mol dm $^{-3}$ ) at the surface of a titanium dioxide nanoparticle ( $1.5 \times 10^{-5}$  mol dm $^{-3}$ ) in the absence and presence of crown ether **10** ( $1 \times 10^{-3}$  mol dm $^{-3}$ ) are shown in the middle panel of Figure 4. No changes were observed in the optical absorption spectrum of **12**·2PF $_6$  adsorbed on titanium dioxide nanoparticles upon addition of **10**.

The corresponding cyclic voltammograms of the nontripodal viologen **12**·2PF $_6$  ( $6 \times 10^{16}$  molecules cm $^{-2}$ ) adsorbed at the surface of the constituent TiO $_2$  nanoparticles of a nanostructured film, in the absence and presence of the crown ether **10** ( $1 \times 10^{-2}$  mol dm $^{-3}$ ), are shown in the bottom panel of Figure 4. It is found that neither the first nor the second peak reduction potential of the viologen is shifted to a more negative value in the presence of the added crown. It is also found that neither the first nor the second peak oxidation potential is shifted to a more negative value in the presence of added crown.

On the basis of the above findings, it may be concluded that the nontripodal viologen **12**·2PF $_6$  does not thread the crown ether **10** to form a pseudorotaxane when adsorbed at the surface of a nanoparticle. On the basis of the above findings, it may also be concluded that the viologen moiety is not adsorbed flat at the surface of the titanium dioxide nanoparticle. Accordingly, one is led to the conclusion that either the viologen moiety in **12**·2PF $_6$  possesses an average orientation with respect to the nanoparticle surface that disfavors complexation or it is sufficiently close to the surface that unfavorable interactions between the crown and the surface dominate and prevent complexation. Studies are ongoing to address this question.

## Conclusion

A tripodal viologen, **9**·2PF $_6$ , has been designed and synthesized that is adsorbed normal to and displaced from the surface of a titanium dioxide nanoparticle in solution. Due to the fact that the tripodal viologen **9** is oriented normal to and displaced from the surface of the titanium dioxide nanoparticle, it possesses the ability to thread the crown **10** to form heteropseudorotaxane.

## Experimental Section

**Synthesis of Tripodal Viologens.** Reagents and solvents were purchased from Aldrich Co. and were used as received. All reactions were performed under nitrogen. The glassware was flame-dried. The chromatography separations were performed with silica (Merck, 40–63  $\mu\text{m}$ ) and the specified solvent system. Melting points were estimated with a Gallenkamp melting point device and were not corrected. NMR spectra were recorded on Varian Inova 300 and 500 spectrometers in the indicated solvent at 30 °C. Proton NMR spectra were recorded at 299.89 and 499.82 MHz, and phosphorus NMR spectra, at 121.39 MHz. Mass spectra were recorded on a Finnigan Mat INCOS 50 quadrupole mass spectrometer.

The viologens 1-{4-[tris[4-(4-dihydrophosphonophenyl)phenyl]methyl]phenyl}-1'-{4-[2-(2-phenoxyethoxy)ethoxy]benzyl}-4,4'-bipyridinium dibromide (**9b**·2Br) and 1-ethyl-1'-phosphonoethyl-4,4'-bipyridinium dibromide (**12**·2Br) and the stabilizers 1-(2-phosphonoethyl)pyridinium bromide (**13**·Br) and the partially deuterated analogue 1-(2-phosphonoethyl)pyridinium- $d_5$  bromide (**14**·Br) were synthesized as shown in Scheme 2.

**Tris[4-(4-bromophenyl)phenyl]methanol (2).** Diethyl ether (12 cm $^3$ ) was added to a solution of **1** (1.56 g, 5 mmol) in THF (12 cm $^3$ ), the mixture was cooled to  $-75$  °C, and *n*-butyllithium (2.4 cm $^3$  of 2.5 mol dm $^{-3}$  in hexane, 6 mmol) was added dropwise over 90 min. The mixture was stirred for 1 h, after which diethyl carbonate (0.14 g, 1.25 mmol) in THF (1 cm $^3$ ) was added slowly. The mixture was allowed to warm to 0 °C (ice bath) and was stirred for 3 h. The mixture was quenched with methanol (1 cm $^3$ ) and the solvent was removed under vacuum. The residue was extracted with ethyl acetate, and the extract was washed with water, dried (MgSO $_4$ ), and concentrated. The oily residue was taken up in chloroform and separated by chromatography (chloroform–hexane). The product **2** (0.40 g; 44%) was isolated as a white solid, mp 166 °C:  $^1\text{H}$  NMR (CDCl $_3$ )  $\delta$  7.59 (d, 6H,  $J$  = 8.5 Hz), 7.56 (d, 6H,  $J$  = 8.5 Hz), 7.48 (d, 6H,  $J$  = 8.5 Hz), 7.46 (d, 6H,  $J$  = 8.5 Hz), 2.88 (s, 1H); MS  $m/z$  726 (M $^+$ ,  $^{81}\text{Br}$ , 100%). Anal. Calcd for C $_{37}$ H $_{25}$ Br $_3$ O: C, 61.27; H, 3.47. Found: C, 61.50; H 3.81.

**4-{Tris[4-(4-bromophenyl)phenyl]methyl}aniline (3).** Acetic acid (12 cm $^3$ ), **2** (0.66 g, 0.9 mmol), and aniline hydrochloride (0.21 g, 1.8 mmol) were added to toluene (4 cm $^3$ ), and the mixture was stirred at 100 °C for 24 h. The solvents were evaporated under vacuum, after which methanol (20 cm $^3$ ) and HCl (2 mol dm $^{-3}$ , 1 cm $^3$ ) were added. The slurry was refluxed for 24 h and the solvent was evaporated under vacuum. The residue was dissolved in chloroform and washed with aqueous NaHCO $_3$ . The chloroform extract was dried (MgSO $_4$ ) and concentrated under vacuum. The residue was purified by chromatography (ethyl acetate–hexane) to give **3** (0.57 g, 78%) as a pale solid; mp 152 °C;  $^1\text{H}$  NMR (CDCl $_3$ )  $\delta$  7.57 (d, 6H,  $J$  = 8.6 Hz), 7.5 (m, 12H), 7.37 (d, 6H,  $J$  = 8.6 Hz), 7.10 (d, 2H,  $J$  = 8.5 Hz), 6.67 (d, 2H,  $J$  = 8.6 Hz); MS  $m/z$  799 (M $^+$ ,  $^{79}\text{Br}$ , 100%). Anal. Calcd for C $_{43}$ H $_{30}$ Br $_3$ N: C, 64.52; H, 3.78; N 1.75. Found: C, 64.55; H, 3.79; N, 1.70.

**4-{Tris[4-(4-(diethoxyphosphono)phenyl]phenyl]methyl}aniline (4).** Compound **3** (0.08 g, 0.1 mmol), acetonitrile (2 cm $^3$ ), and diethyl phosphite (0.25 cm $^3$ , 0.28 g, 2 mmol) were added to dry potassium carbonate (0.14 g, 1 mmol) followed by bis-1,1'-(diphenylphosphino)ferrocenedichloropalladium complex with dichloromethane (0.005 g, 0.006 mmol). The mixture was heated under reflux for 15 h, after which time additional palladium catalyst (0.005 g) was added. The mixture was refluxed for 20 h, filtered (the precipitate was washed with an excess of acetone), and concentrated under vacuum. The residue was purified by chromatography on silica gel (10% MeOH in acetone) to give **4** (0.062 g; 63%) as a solid: mp 132 °C;  $^1\text{H}$  NMR (CDCl $_3$ )  $\delta$  7.89 (dd, 6H,  $J$  = 8.5, 13 Hz), 7.71 (dd, 6H,  $J$  = 8.5, 4 Hz), 7.56 (d, 6H,  $J$  = 8.6 Hz), 7.41 (d, 6H,  $J$  = 8.6 Hz), 7.09 (d, 2H,  $J$  = 8.6 Hz), 6.66 (d, 2H,  $J$  = 8.6 Hz), 4.1–4.3 (m, 12H), 1.36 (t, 18H,  $J$  = 7 Hz);  $^{31}\text{P}$  NMR (CDCl $_3$ )  $\delta$  19.96; MS  $m/z$  971 (M $^+$ , 100%). Anal. Calcd for C $_{55}$ H $_{60}$ NO $_9$ P $_3$ : C, 67.96; H, 6.22; N, 1.44. Found: C, 67.55; H, 6.03; N, 1.60.

**1-(2,4-Dinitrophenyl)-4,4'-bipyridinium chloride (5)** was obtained as reported.<sup>14</sup>

**1-[4-[Tris[4-[4-(diethoxyphosphono)phenyl]phenyl]methyl]phenyl]-4,4'-bipyridinium Chloride (6·Cl)**. Compound **5** (0.18 g 0.5 mmol) and dry ethanol (10 cm<sup>3</sup>) were added to **4** (0.35 g, 0.36 mmol), and the mixture was heated under reflux for 30 h. The solvent was evaporated under vacuum. The residue was dissolved in chloroform (100 cm<sup>3</sup>) and washed with water (50 cm<sup>3</sup>) to remove excess **5**. The organic layer was dried (MgSO<sub>4</sub>) and concentrated. The residue was taken up in acetone and purified by chromatography (methanol–acetic acid) to give the product **6·Cl** (0.35 g, 85%) as a yellowish glassy solid: <sup>1</sup>H NMR (CD<sub>3</sub>OD) δ 9.46 (d, 2H, *J* = 6 Hz), 8.98 (br s, 2H), 8.74 (d, 2H, *J* = 6 Hz), 8.26 (d, 2H, *J* = 6 Hz), 7.8–7.9 (m, 16H), 7.74 (dd, 6H, *J* = 8.5, 4 Hz), 7.55 (d, 6H, *J* = 8.6 Hz), 4.1–4.3 (m, 12H), 1.36 (t, 18H, *J* = 7 Hz); <sup>31</sup>P NMR (CD<sub>3</sub>OD) δ 20.32.

The solubility of the 4,4'-bipyridinium monocation **6** depends strongly upon the counterion of the salt. Since it was found that the hexafluorophosphates are more soluble in suitable solvents and could be purified more readily,<sup>6</sup> these salts were used in all subsequent transformations.

**1-[4-[Tris[4-[4-(diethoxyphosphono)phenyl]phenyl]methyl]phenyl]-4,4'-bipyridinium Hexafluorophosphate (6·PF<sub>6</sub>)**. An aqueous solution of NH<sub>4</sub>PF<sub>6</sub> (2 M, 1 cm<sup>3</sup>) was added to a solution of **6·Cl** (0.100 g, 0.085 mmol) in chloroform (50 cm<sup>3</sup>). The mixture was shaken for 1 min, and the organic layer was dried (Na<sub>2</sub>SO<sub>4</sub>) and concentrated to give **6·PF<sub>6</sub>** (0.100 g, 93%) as a yellow solid: mp 210–220 °C (decomp); <sup>1</sup>H NMR (CD<sub>3</sub>OD) δ 8.84 (d, 2H, *J* = 6 Hz), 8.66 (d, 2H, *J* = 5 Hz), 8.29 (d, 2H, *J* = 6 Hz), 7.7–7.9 (m, 6H), 7.6 (m, 12H), 7.50 (d, 6H, *J* = 8.5 Hz), 7.33 (d, 6H, *J* = 8.6 Hz), 4.0–4.2 (m, 12H), 1.25 (t, 18H, *J* = 7 Hz); <sup>31</sup>P NMR (CD<sub>3</sub>OD) δ 19.74 (s), –143.46 (heptet, *J* = 711 Hz); MS *m/z* 1111 (**6**<sup>+</sup>, 100%). Anal. Calcd for C<sub>65</sub>H<sub>66</sub>F<sub>6</sub>N<sub>2</sub>O<sub>9</sub>P<sub>4</sub>: C, 62.10; H, 5.29; N, 2.23. Found: C, 61.90; H, 5.17; N, 2.11.

**1-[4-[Tris[4-[4-(diethoxyphosphono)phenyl]phenyl]methyl]phenyl]-1'-ethyl-4,4'-bipyridinium Bis(hexafluorophosphate) (8a·2PF<sub>6</sub>)**. Acetonitrile (1 cm<sup>3</sup>) and ethyl bromide **7a** (0.6 g, 5 mmol) were added to **6·PF<sub>6</sub>** (0.025 g, 0.02 mmol), and the mixture was heated at 80 °C in a sealed tube for 24 h. The mixture was concentrated and the product was purified by chromatography [methanol–nitromethane–aqueous NH<sub>4</sub>PF<sub>6</sub> (2 mol dm<sup>-3</sup>) in the ratio 80:19:1 by volume] to give **8a·2PF<sub>6</sub>** (0.027 g, 95%) as a yellow solid: mp 210–220 °C (decomposition); <sup>1</sup>H NMR (CD<sub>3</sub>OD) δ 9.07 (d, 2H, *J* = 7 Hz), 8.95 (d, 2H, *J* = 6.4 Hz), 8.55 (d, 2H, *J* = 7 Hz), 8.43 (d, 2H, *J* = 6.4 Hz), 7.6–7.9 (m, 16H), 7.53 (d, 6H, *J* = 8.5 Hz), 7.35 (d, 6H, *J* = 8.5 Hz), 4.63 (q, 2H, *J* = 7.2 Hz), 4.0–4.2 (m, 12H), 1.63 (t, 3H, *J* = 7.2 Hz), 1.26 (t, 18H, *J* = 7 Hz); <sup>31</sup>P NMR (CD<sub>3</sub>OD) δ 20.24 (s), –143.68 (heptet); MS *m/z* 1139 (**8a**<sup>+</sup> – H, 92%), 570 (**8a**<sup>2+</sup>, 100%). Anal. Calcd for C<sub>67</sub>H<sub>71</sub>F<sub>12</sub>N<sub>2</sub>O<sub>9</sub>P<sub>5</sub>: C, 56.23; H, 5.00; N, 1.96. Found: C, 55.88; H, 4.75; N, 1.92.

**4-[2-(2-Phenoxyethoxy)ethoxy]benzyl Bromide (7b)** was obtained similarly to the procedure reported.<sup>13</sup> Colorless solid: mp 58 °C; <sup>1</sup>H NMR (CD<sub>3</sub>OD) δ 7.2–7.35 (m, 4H), 6.8–7.0 (d, 5H, *J* = 8.5 Hz), 4.42 (s, 2H), 4.08 (t, 4H, *J* = 5 Hz), 3.85 (t, 4H, *J* = 5 Hz). Anal. Calcd for C<sub>17</sub>H<sub>19</sub>BrO<sub>3</sub>: C, 58.10; H, 5.45; Br, 22.75. Found C, 57.90; H, 5.55; Br, 22.87.

**1-[4-[Tris[4-[4-(diethoxyphosphono)phenyl]phenyl]methyl]phenyl]-1'-[4-[2-(2-phenoxyethoxy)ethoxy]benzyl]-4,4'-bipyridinium Bis(hexafluorophosphate) (8b·2PF<sub>6</sub>)**. Compound **7b** (0.017 g, 0.05 mmol) and benzonitrile (0.1 cm<sup>3</sup>) were added to **6·PF<sub>6</sub>** (0.025 g, 0.02 mmol), and the mixture was heated at 30 °C for 1 day. The crude mixture was purified by chromatography (MeOH/MeNO<sub>2</sub>/NH<sub>4</sub>PF<sub>6</sub>) to give the product **8b·2PF<sub>6</sub>** (0.033 g, 99%) as a bright yellow solid: mp 118 °C; <sup>1</sup>H NMR (CDCl<sub>3</sub>-CD<sub>3</sub>OD) δ 8.99 (d, 2H, *J* = 7 Hz), 8.81 (d, 2H, *J* = 7 Hz), 8.43 (d, 2H, *J* = 7 Hz), 8.31 (d, 2H, *J* = 7 Hz), 7.8 (m, 6H), 7.6 (m, 10H), 7.53 (d, 6H, *J* = 9 Hz), 7.35 (m, 8H), 7.15 (t, 2H, *J* = 7 Hz), 6.75–6.9 (m, 5H), 5.63 (s, 2H), 4.1 (m, 16H), 3.8 (m, 4H), 1.26

(t, 18H, *J* = 7 Hz); <sup>31</sup>P NMR (CDCl<sub>3</sub>-CD<sub>3</sub>OD) δ 20.19 (s), –143.6 (heptet, *J* = 711 Hz); MS (ES) *m/z* 1382 (**8b**<sup>+</sup>, 7%). Anal. Calcd for C<sub>82</sub>H<sub>85</sub>F<sub>12</sub>N<sub>2</sub>O<sub>12</sub>P<sub>5</sub>: C, 58.85; H, 5.12; N, 1.67. Found: C, 58.12; H, 5.02; N, 1.54.

**1-[4-[Tris[4-[4-(dihydrophosphono)phenyl]phenyl]methyl]phenyl]-1'-[4-[2-(2-phenoxyethoxy)ethoxy]benzyl]-4,4'-bipyridinium Dibromide (9·2Br)**. Me<sub>3</sub>SiBr (0.1 cm<sup>3</sup>, 0.75 mmol) was added to **8b·2PF<sub>6</sub>** (0.033 g, 0.02 mmol) in 1,4-dioxane (2 cm<sup>3</sup>), and the mixture was heated at 30 °C for 1 day, after which it was concentrated under vacuum. Water (0.5 cm<sup>3</sup>) and 1,4-dioxane (1.5 cm<sup>3</sup>) were added to the mixture and then removed under reduced pressure. The crude mixture was extracted with methanol to give the product (0.026 g, 95%) as a yellow glass: <sup>1</sup>H NMR (CDCl<sub>3</sub>-CD<sub>3</sub>OD) δ 9.36 (d, 2H, *J* = 6 Hz), 9.20 (d, 2H, *J* = 6 Hz), 8.90 (d, 2H, *J* = 6 Hz), 8.78 (d, 2H, *J* = 6 Hz), 7.8 (m, 6H), 7.6 (m, 10H), 7.5 (m, 8H), 7.4 (m, 6H), 7.18 (t, 2H, 7 Hz), 6.7–7.0 (m, 5H), 5.81 (s, 2H), 4.1 (m, 4H), 3.8 (m, 4H); <sup>31</sup>P NMR (CDCl<sub>3</sub>-CD<sub>3</sub>OD) δ 18.1; MS *m/z* 1212 (**9**<sup>+</sup>, 16%).

**Bis(p-phenylene)-34-crown-10 (10)** was prepared according to the procedure reported:<sup>27</sup> mp 90 °C (lit.<sup>20</sup> mp 88 °C).

**1-Ethyl-1'-(diethylphosphono)ethyl-4,4'-bipyridinium bromide (11·2Br) and 1-ethyl-1'-phosphonoethyl-4,4'-bipyridinium bromide (12·2Br)** were prepared as previously reported.<sup>21</sup>

**1-(2-Phosphonoethyl)pyridinium Bromide (13·Br)**. Pyridine (3 cm<sup>3</sup>) was added to diethyl 2-bromoethylphosphonate (0.98 g, 4 mmol) in acetonitrile (20 cm<sup>3</sup>), and the mixture was heated at 70 °C for 20 h. The mixture was concentrated under reduced pressure, dissolved in water (20 cm<sup>3</sup>), and washed with dichloromethane (2 × 20 cm<sup>3</sup>). The aqueous layer was concentrated and the residue was dissolved in HCl (6 mol dm<sup>-3</sup>, 20 cm<sup>3</sup>). The mixture was heated under reflux for 20 h and evaporated under reduced pressure to give **13·Br** (0.73 g, 65%) as a white solid: mp 152 °C; <sup>1</sup>H NMR (CD<sub>3</sub>OD) δ 9.09 (d, 2H, *J* = 6 Hz), 8.67 (t, 1H, *J* = 7 Hz), 8.16 (m, 2H), 4.92 (q, 2H, *J* = 7 Hz), 4.8 (s, 2H), 2.6 (m, 2H); <sup>31</sup>P NMR (CD<sub>3</sub>OD) δ 25.2 (s). Anal. Calcd for C<sub>7</sub>H<sub>11</sub>BrNO<sub>3</sub>P: C, 31.37; H, 4.14; N, 5.23; Br, 29.81. Found: C, 31.19; H, 3.97; N, 5.16; Br, 29.81.

**1-(2-Phosphonoethyl)perdeuteriopyridinium Bromide (14·Br)**. Pyridine-*d*<sub>5</sub> (0.336 g, 4 mmol) was added to diethyl 2-bromoethylphosphonate (1.22 g, 5 mmol) in acetonitrile (5 cm<sup>3</sup>), and the mixture was heated under reflux for 25 h. The mixture was concentrated under reduced pressure, dissolved in water (20 cm<sup>3</sup>), and washed with dichloromethane (2 × 20 cm<sup>3</sup>). The aqueous layer was concentrated and the residue was dissolved in HCl (6 mol dm<sup>-3</sup>, 10 cm<sup>3</sup>). The mixture was heated under reflux for 20 h and evaporated under reduced pressure to give **14·Br** (0.88 g, 80%) as a white solid: mp 154 °C; <sup>1</sup>H NMR (CD<sub>3</sub>OD) δ 9.09 (trace), 8.67 (trace), 8.16 (trace), 4.92 (q, 2H, *J* = 7 Hz), 4.8 (s, 2H, exchangeable signal), 2.6 (m, 2H); <sup>31</sup>P NMR (CD<sub>3</sub>OD) δ 22.1 (s). Anal. Calcd for C<sub>7</sub>H<sub>6</sub>D<sub>5</sub>BrNO<sub>3</sub>P: C, 30.79; H, 5.90; N, 5.13; Br, 29.26. Found: C, 31.15; H, 5.96; N, 5.16; Br, 29.08.

**Determination of Association Constants.** The method used to determine *K*<sub>a</sub> was developed by Ray and adapted by Stoddart for pseudorotaxanes.<sup>15,16</sup> It involves measuring the optical absorption spectrum of different solutions containing equal concentrations of, for example, the viologen **8b·2PF<sub>6</sub>** and the crown ether **10**. This method assumes that the complex formed has a 1:1 stoichiometry and allows *K*<sub>a</sub> to be defined as

$$K_a = \frac{[\mathbf{8b} \cdot \mathbf{10} \cdot 2\text{PF}_6]}{[\mathbf{8b} \cdot 2\text{PF}_6][\mathbf{10}]} \quad (1)$$

(27) Anelli, P. L.; Ashton, P. R.; Ballardini, R.; Balzani, V.; Delgado, M.; Gandolfi, M. T.; Goodnow, T. T.; Kaifer, A. E.; Philp, D.; Pietraszkiewicz, M.; Prodi, L.; Reddington, M. V.; Slavin, A. M. Z.; Spencer, N.; Stoddart, J. F.; Vincenti, C.; Williams, D. J. *J. Am. Chem. Soc.* **1992**, *114*, 193–218.

(28) Rao, S. N.; Fitzmaurice, D. *Helv. Chim. Acta* **1998**, *81* (5), 902.



A series of refinements to eq 1 leads to a plot of  $c/A$  against  $1/(A)^{1/2}$  according to

$$\frac{c}{A} = \frac{1}{(K_a \epsilon l)^{1/2}} \frac{1}{(A)^{1/2}} + \frac{1}{\epsilon l} \quad (2)$$

$A$  is the absorbance of the complex at  $\lambda_{\max}$ ,  $c$  is the concentration of the viologen and of the crown ether,  $\epsilon$  is the extinction coefficient of the CT band, and  $l$  is the optical path length, which is 1 cm. The slope of a plot of  $c/A$  against  $1/(A)^{1/2}$  yields  $(1/K_a \epsilon l)^{1/2}$ , while the intercept of the same plot yields  $(1/\epsilon l)$ .

All optical absorption spectra were recorded at 25 °C on a Hewlett-Packard 8452A diode array spectrometer controlled by a LabView program running on a Macintosh Power PC. A standard solution containing equimolar amounts of **8b**·2PF<sub>6</sub> and **10** ( $8 \times 10^{-3}$  mol dm<sup>-3</sup>) in a 2 cm<sup>3</sup> volumetric flask was prepared. The absorption spectrum of the standard solution was recorded and the absorbance at  $\lambda_{\max}$  was determined. The solution was diluted accurately and the solution's new absorbance was measured. This process of dilution and measurement was repeated. In total, 15 data points were obtained. Accurate dilution factors and concentrations were determined gravimetrically for the above solutions. Association constants,  $K_a$ , and derived free energies of complexation,  $-\Delta G^\circ$ , were obtained. Complexation of the nontripodal viologen **11**·2Br with crown ether **10** was also studied by the same method.

**Preparation of an Aqueous Dispersion of Titanium Dioxide Nanoparticles.** An aqueous dispersion of titanium dioxide nanoparticles was prepared as previously reported by hydrolysis of titanium tetraisopropoxide at pH 2.<sup>19</sup> Heating for 8 h evaporates the unwanted side product 2-propanol and promotes crystallization of the nanoparticles. The average diameter of the TiO<sub>2</sub> particles was determined to be 5 nm by TEM. X-ray diffraction confirmed that the crystal structure was anatase. The final concentration of TiO<sub>2</sub> as determined by dry weight measurements was 3.2% (w/w).

**Preparation of Modified Nanoparticles.** An aqueous dispersion of TiO<sub>2</sub> nanoparticles (1 cm<sup>3</sup>) was transferred to a centrifuge tube and was diluted with methanol (to 10 cm<sup>3</sup>). Viologen **9**·2Br (3.2 mg, 2 μmol) or **12**·2Br (0.9 mg, 2 μmol) in CHCl<sub>3</sub>/MeOH (1:1 v/v) was added dropwise to a vigorously stirred solution of TiO<sub>2</sub>. This was stirred for a further 10 min after addition was completed. Either **13**·Br or **14**·Br (10 mg, 30 μmol) in MeOH (1 cm<sup>3</sup>) was added to this solution, which was then stirred for 1 h. To induce counterion exchange and precipitation, NH<sub>4</sub>PF<sub>6</sub> was added in large excess (0.1 mmol). The precipitate was centrifuged and washed with dry MeOH (5 cm<sup>3</sup>). The last step was repeated three times to remove all the residual water. Finally the precipitate is then transferred into acetonitrile (3 cm<sup>3</sup>) and sonicated for 1 h to redisperse the particles. The resulting solution is an optically transparent dispersion of modified TiO<sub>2</sub> nanoparticles.

**Preparation of Transparent Nanostructured TiO<sub>2</sub> Films.** Transparent nanostructured TiO<sub>2</sub> films were deposited on F-doped tin oxide glass substrates (10 Ω units, 0.5 μm thick, supplied by Glastron). Specifically, a colloidal dispersion of TiO<sub>2</sub> was prepared as described above. It was then autoclaved at 200 °C for 12 h to yield a dispersion of 12 nm diameter nanocrystals. Concentration of this dispersion (160 g L<sup>-1</sup>) and addition of Carbowax 20000 (40 wt % equivalent of TiO<sub>2</sub>) yields a viscous paste. This paste was spread with a glass rod on the conducting glass substrate masked by scotch tape. Following drying in air for 1 h, the film was fired, also in air at 450 °C for 12 h. The resulting transparent nanostructured electrodes are 4 μm thick.

**Modification of Transparent Nanostructured TiO<sub>2</sub> Films.** A transparent nanostructured TiO<sub>2</sub> film was immersed in a dry acetonitrile solution of the required molecular component (0.5 mmol) for 1 h at room temperature. The modified film was removed from the above solution, washed thoroughly with dry acetonitrile, and stored in a desiccator until required for use. The active area of the film is 0.8 cm<sup>2</sup> (geometric area) × 1000 (surface roughness), which is 800 cm<sup>2</sup>. The density of sites at which a phosphonate linker may be adsorbed is  $2 \times 10^{14}$  cm<sup>-2</sup>.<sup>25</sup> On this basis it is estimated that there are approximately  $5 \times 10^{16}$  tripodal viologens and  $1.5 \times 10^{17}$  nontripodal viologens adsorbed at the surface of the TiO<sub>2</sub> film.

**Electrochemical Characterization.** All cyclic voltammograms were recorded in solution under the following conditions: The working electrode (WE) was an isolated platinum wire. The counterelectrode (CE) was an isolated platinum gauze. The reference electrode (RE) was a nonaqueous Ag/Ag<sup>+</sup> electrode filled with 10 mM AgNO<sub>3</sub> in the electrolyte solution. The electrolyte solution consisted of 0.1 M tetrabutylammonium perchlorate (TBAP) in dry acetonitrile. When stated, a 5-fold excess of crown ether was added to all viologen samples, thereby ensuring that virtually all the viologen was present in the complexed form. The solutions were bubbled with argon gas for 20 min prior to measurement. All cyclic voltammograms were recorded on a Solartron SI 1287 potentiostat controlled by a LabView program running on a Macintosh Power PC at a scan rate of 20 mV s<sup>-1</sup> unless otherwise stated.

All cyclic voltammograms were recorded for nanostructured TiO<sub>2</sub> films under the following conditions: The working electrode (WE) was a nanostructured TiO<sub>2</sub> film. The counterelectrode (CE) was isolated platinum gauze. The reference electrode (RE) was a nonaqueous Ag/Ag<sup>+</sup> electrode filled with 10 mM AgNO<sub>3</sub> in the electrolyte solution. The electrolyte solution consisted of 0.1 M TBAP in dry acetonitrile. When stated, a 10 mM solution of crown ether was added to the electrolyte solution. The solutions were rigorously degassed by the freeze-thaw method under nitrogen gas. As above, all cyclic voltammograms were recorded on a Solartron SI 1287 potentiostat controlled by a LabView program running on a Macintosh Power PC at a scan rate of 20 mV s<sup>-1</sup> unless otherwise stated.

JA028870Z